SOFTWARE NOTE

FlowerMate: Multidimensional reciprocity and inaccuracy indices for style-polymorphic plant populations

Violeta Simón-Porcar[1,2] | **A. Jesús Muñoz-Pajares**[3,4] | **Juan Arroyo**[1] | **Steven D. Johnson**[2]

[1]Department of Plant Biology and Ecology, University of Seville, Seville E-41080, Spain

[2]Centre for Functional Biodiversity, School of Life Sciences, University of KwaZulu-Natal, Pietermaritzburg 3209, South Africa

[3]Department of Genetics, University of Granada, Granada E-18071, Spain

[4]Research Unit Modeling Nature, University of Granada, Granada E-18071, Spain

Correspondence

Violeta Simón-Porcar, Department of Plant Biology and Ecology, University of Seville, E-41080 Seville, Spain.
Email: violetasp@us.es

Abstract

Premise: Heterostyly in plants promotes pollen transfer between floral morphs, because female and male sex organs are located at roughly reciprocal heights within the flowers of each morph. Reciprocity indices, which assess the one-dimensional variation in the height of sex organs, are used to define the phenotypic structure of heterostyly in plant populations and to make inferences about selection. Other reciprocal stylar polymorphisms (e.g., enantiostyly) may function in a similar manner to heterostyly. In-depth assessment of their potential fit with pollinators requires accounting for the multidimensional variation in the location of sex organs.

Methods and Results: We have adapted the existing reciprocity indices used for heterostylous plant populations to incorporate multidimensional data. We illustrate the computation of the adapted and original indices in the freely available R package FlowerMate.

Conclusions: FlowerMate provides fast computation of reliable indices to facilitate understanding of the evolution and function of the full diversity of reciprocal polymorphisms.

KEYWORDS

FlowerMate, heterostyly, inaccuracy, reciprocal polymorphism, reciprocity, stylar polymorphism

Assessing phenotypic variation in natural populations is a fundamental component of evolutionary ecology (Fox et al., 2001), and the development of biological metrics that appropriately represent such variation is thus crucial. Although fitness measures are key for testing natural selection, reduced phenotypic variation has also been regarded as an indication of the strength of long-term directional or stabilizing selection (Fisher, 1958; Lande and Arnold, 1983; Fenster, 1991; Cresswell, 1998).

Heterostylous plants are a classical model system to test evolution by natural selection (Darwin, 1877; Barrett, 2019). Typical heterostylous plants present polymorphic populations with two (distyly) or three (tristyly) floral morphs bearing stigmas and anthers at different and roughly reciprocal heights. The polymorphism may function for efficient transfer of pollen between morphs

on different parts of a pollinator's body (Darwin, 1877; e.g. Massinga et al., 2005), and this may depend on the exact reciprocity in the height of sex organs (Ferrero et al., 2011a; Brys and Jacquemyn, 2020; Simón-Porcar et al., 2022). In consequence, morph ratios may be directly related to reciprocity, particularly in heterostylous plants without heteromorphic incompatibility (Thompson et al., 2012).

Reciprocity indices have been a common approach for defining the phenotypic structure of heterostyly in plant populations (e.g., Richards and Koptur, 1993; Eckert and Barrett, 1994; Faife-Cabrera et al., 2014; Oliveira et al., 2022) and for analyzing their correlates with plant fitness to test natural selection (e.g., Faife-Cabrera et al., 2018; Jacquemyn et al., 2018; Ganguly and Barua, 2021; Ganguly et al., 2021). Two indices that have been used

extensively in the past decade to assess the extent of reciprocity in populations are the reciprocity index of Sánchez et al. (2008, 2013) and the inaccuracy index of Armbruster et al. (2017). Calculating these indices has involved manual or spreadsheet computations, which may be prone to error and time consuming when handling large databases.

Reciprocity indices can be extended to include three-dimensional forms of heterostyly (Armbruster et al., 2006; Turketti et al., 2012; Rech et al., 2020) and other stylar polymorphisms such as enantiostyly (Barrett, 2002), flexistyly (Li et al., 2001), inversostyly (Pauw, 2005), or resupinate dimorphy (Harley et al., 2017). These polymorphisms, with a relatively constant fit of pollinators seeking nectar, can result in disassortative pollen transfer in a similar manner to heterostyly (e.g., Minnaar and Anderson, 2021; Johnson et al., 2023) and are thus appropriate for the application of reciprocity indices (e.g., Braga et al., 2022). In these cases, reciprocity indices must account for the multidimensional variation in the location of sex organs, as this ultimately determines their contact with pollinator bodies.

We adapted the reciprocity (Sánchez et al., 2008, 2013) and inaccuracy (Armbruster et al., 2017) indices for multidimensional data. Both the adapted and the original indices are implemented in the R package FlowerMate (Muñoz-Pajares and Simón-Porcar, 2024), which also includes various automated functions for data handling in a flexible environment that accommodates virtually any type of stylar polymorphism.

METHODS AND RESULTS

Adaptation of the reciprocity index for heterostylous populations to multidimensional data

Below, we replicate and complete the mathematical formulation for the reciprocity index for distylous plant populations of Sánchez et al. (2008, 2013) and show the modifications applied to incorporate multidimensional data. Symbols and all abbreviations used in the following equations are summarized and described in Table 1.

First, Sánchez et al. (2008) averaged the heights of all sex organs (stigmas and anthers) in the population. To avoid over-representation of anthers in comparison with stigmas (of which there is frequently only one), this value was calculated as the average of the mean number of anthers and the mean number of stigmas.

$$\overline{X} = \frac{1}{2}\left(\frac{\sum_i^n \sum_k^p (E_i + e_k)}{n + p} + \frac{\sum_j^m \sum_v^q (S_j + s_v)}{m + q}\right) \quad (1)$$

Second, the authors averaged the height gaps (stigma–anther distances) of all possible crosses (i.e., individual

TABLE 1 List of abbreviations used in the mathematical formulations.

Abbreviation	Definition
E	Stamen height at level L (long), i.e., in flowers of morph-A plants
S	Stigma height at level L, i.e., in flowers of morph-B plants
e	Stamen height at level S (short), i.e., in flowers of morph-A plants
s	Stigma height at level S, i.e., in flowers of morph-B plants
n	Total number of all single stamens (i) at level L
m	Total number of all single stigmas (j) at level L
p	Total number of all single stamens (l) at level S
q	Total number of all single stigmas (k) at level S
r_a	Mean relative reciprocity at level a (Sánchez et al., 2008)
$\overline{X}$	Weighted average of heights of all organs (stigmas and stamens) in the population
R	Reciprocity index, following Sánchez et al. (2013)
r	Overall reciprocity of the population
r_L	Relative reciprocity at level L
r_S	Relative reciprocity at level S
sdr	Overall standard deviation of the height gaps in the population
sdr_a	Standard deviation of the height gaps at level a
sdr_L	Standard deviation of height gaps at level L
sdr_S	Standard deviation of height gaps at level S
r_{a3D}	Mean relative 3D reciprocity at level a
$\overline{X}_{3D}$	Average of 3D heights of all organs (stigmas and stamens) in the population
$\overline{A}$	Average height of anthers at upper level
$\overline{S}$	Average height of stigmas at upper level
$\overline{a}$	Average height of anthers at lower level
$\overline{s}$	Average height of stigmas at lower level
V_A	Variance in the height of anthers at upper level
V_S	Variance in the height of stigmas at upper level
V_a	Variance in the height of anthers at lower level
V_s	Variance in the height of stigmas at lower level
M^2STI	Mean²-standardized total inaccuracy
$PADO$	Population average distance to the origin
T	Total number of sex organs measured

mating pairs) in the population at each height level (where L represents the upper level and S the lower level), using the $\overline{X}$ value to standardize the stigma–anther distances across populations, to obtain the mean relative reciprocities at each level:

$$r_L = \frac{1}{nm}\left(\sum_i^n \sum_j^m \left(\frac{|E_i - S_j|}{\overline{X}}\right)\right) \quad (2a)$$

$$r_S = \frac{1}{pq}\left(\sum_k^p \sum_v^q \left(\frac{|e_k - s_v|}{\overline{X}}\right)\right) \quad (2b)$$

and the overall reciprocity in a population as the Euclidean distance from zero to the population's location in a bivariate space defined by the two relative reciprocity indices:

$$r = \sqrt{(r_L)^2 + (r_S)^2} \quad (3)$$

Third, they calculated the average standard deviation of height gaps among sex organs at each level:

$$sdr_L = \sqrt{\left[\frac{1}{nm}\left(\sum_i^n \sum_j^m \left[\left(\frac{|E_i - S_j|}{\overline{X}}\right) - r_L\right]^2\right)\right]} \quad (4a)$$

$$sdr_S = \sqrt{\left[\frac{1}{pq}\left(\sum_k^p \sum_v^q \left[\left(\frac{|e_k - s_v|}{\overline{X}}\right) - r_S\right]^2\right)\right]} \quad (4b)$$

and averaged them to obtain the overall standard deviation:

$$sdr = \frac{1}{2}(sdr_L + sdr_S) \quad (5)$$

Finally, the reciprocity index, following the modification of Sánchez et al. (2013) was calculated as:

$$R = 1 - (10r \times sdr) \quad (6)$$

R equals one in situations of perfect reciprocity and decreases as variance and mismatches between corresponding sex organs increase. Remarkably, the index can potentially take on negative values, although Sánchez et al. (2013) did not discuss this.

The basis of the adaptation of the reciprocity index to multidimensional data was substituting sex organ height (i.e., distances along the y-axis) with distances in a virtual three-dimensional (3D) space; i.e.,

$$\sqrt{(x_2 - x_1)^2 + (y_2 - y_1)^2 + (z_2 - z_1)^2} \quad (7)$$

Hence, the heights of sex organs were substituted with their distances to the origin in a 3D space (e.g., for a stamen at level L):

$$\sqrt{(x_{E_i})^2 + (y_{E_i})^2 + (z_{E_i})^2} \quad (8)$$

and the distance for a stigma–stamen pair was calculated (e.g., at level L) as:

$$\sqrt{\left(x_{E_i} - x_{S_j}\right)^2 + \left(y_{E_i} - y_{S_j}\right)^2 + \left(z_{E_i} - z_{S_j}\right)^2} \quad (9)$$

Although we only provide formulation for three dimensions, setting coordinates to zero in one or two dimensions would lead to the corresponding index in two-dimensional or one-dimensional space (the original index of Sánchez et al., 2008, 2013), respectively. For the sake of clarity, we maintain the "L" and "S" nomenclature of sex organ levels of distylous species, although as explained above these indices may apply to other types of stylar morphs.

To adapt the reciprocity index, we first substituted sex organ height in Eq. 1 with their distances to the origin (Eq. 8).

$$\bar{X}_{3D} = \frac{1}{2}\left[\frac{\sum_i^n \sum_k^p \left(\sqrt{(x_{E_i})^2 + (y_{E_i})^2 + (z_{E_i})^2} + \sqrt{(x_{e_k})^2 + (y_{e_k})^2 + (z_{e_k})^2}\right)}{n + p} + \frac{\sum_j^m \sum_v^q \left(\sqrt{(x_{S_j})^2 + (y_{S_j})^2 + (z_{S_j})^2} + \sqrt{(x_{s_v})^2 + (y_{s_v})^2 + (z_{s_v})^2}\right)}{m + q}\right] \quad (10)$$

Second, we computed the mean relative reciprocity at each level, following Eq. 2a, 2b, and 9:

$$r_{L3D} = \frac{1}{nm}\left(\sum_i^n \sum_j^m \left(\frac{\sqrt{\left(x_{E_i} - x_{S_j}\right)^2 + \left(y_{E_i} - y_{S_j}\right)^2 + \left(z_{E_i} - z_{S_j}\right)^2}}{\bar{X}_{3D}}\right)\right) \quad (11a)$$

$$r_{S3D} = \frac{1}{pq}\left(\sum_k^p \sum_v^q \left(\frac{\sqrt{\left(x_{e_k} - x_{s_v}\right)^2 + \left(y_{e_k} - y_{s_v}\right)^2 + \left(z_{e_k} - z_{s_v}\right)^2}}{\bar{X}_{3D}}\right)\right) \quad (11b)$$

and the overall 3D reciprocity in the population, following Eq. 3:

$$r_{3D} = \sqrt{(r_{L3D})^2 + (r_{S3D})^2} \quad (12)$$

Third, we computed the average standard deviation of 3D distances among sex organs at each level, following Eq. 4a, 4b, and 9:

sdr_{L3D}

$$= \sqrt{\left[\frac{1}{nm}\sum_i^n\sum_j^m\left[\left[\left(\frac{\sqrt{\left(x_{E_i} - x_{S_j}\right)^2 + \left(y_{E_i} - y_{S_j}\right)^2 + \left(z_{E_i} - z_{S_j}\right)^2}}{\overline{X}_{3D}}\right) - r_{L3D}\right]^2\right]\right]}$$

(13a)

sdr_{S3D}

$$= \sqrt{\left[\frac{1}{pq}\sum_k^p\sum_v^q\left[\left[\left(\frac{\sqrt{\left(x_{e_k} - x_{s_v}\right)^2 + \left(y_{e_k} - y_{s_v}\right)^2 + \left(z_{e_k} - z_{s_v}\right)^2}}{\overline{X}_{3D}}\right) - r_{S3D}\right]^2\right]\right]}$$

(13b)

and the overall average standard deviation following Eq. 5:

$$sdr_{3D} = \frac{1}{2}(sdr_{L3D} + sdr_{S3D}) \qquad (14)$$

Finally, the 3D reciprocity index, following Eq. 6, was defined as:

$$R_{3D} = 1 - (10 r_{3D} \times sdr_{3D}) \qquad (15)$$

Sánchez et al. (2013) applied their reciprocity index to tristylous plant populations by computing r_L, r_S, and r_M (for the mid-level sex organs) as in Eq. 2, and by computing the overall reciprocity in a population as the mean value of the Euclidean distances from zero to each value of relative reciprocity in each one of the three two-dimensional spaces defined by the three levels:

$$r = \frac{1}{3}\left(\sqrt{(r_L)^2 + (r_S)^2} + \sqrt{(r_L)^2 + (r_M)^2} + \sqrt{(r_M)^2 + (r_S)^2}\right)$$

(16)

Similarly, they computed sdr_L, sdr_S, and sdr_M as in Eq. 4, and the overall standard deviation as their average value:

$$sdr = \frac{1}{3}(sdr_L + sdr_S + sdr_M) \qquad (17)$$

Their final reciprocity index for tristylous populations was calculated as in Eq. 6, using the values for r and sdr provided in Eq. 16 and 17.

We applied the same modifications in Eq. 11 to 15 to compute a multidimensional reciprocity index for trimorphic populations (notably, so far only reported in heterostylous systems and not in other reciprocal stylar polymorphisms).

Computation of the inaccuracy index for multidimensional data

Adaptive inaccuracy is a comprehensive conceptual framework for estimating the fitness consequences of population or individual plant-level deviations from morphological fitness optima (Armbruster et al., 2009a, 2009b; Pélabon et al., 2012). We acknowledge that this framework is beyond the concept of "index," as applied here for the sake of simplicity. Armbruster et al. (2017) defined the inaccuracy for heterostylous flowers in the context of the adaptive inaccuracy of a morph on a fitness scale. Below, we replicate and complete the mathematical formulation for the inaccuracy index of Armbruster et al. (2017) and show the modifications applied to incorporate multidimensional data. Symbols and all abbreviations used in the following equations are summarized and described in Table 1.

Armbruster et al. (2017) defined inaccuracy of heterostylous populations giving the same weight to both the maladaptive bias (mean departure from optimum) and imprecision (within-population variance) of the phenotypic values in the population. Accordingly, they defined the following parameters:

$$\text{Inaccuracy}_{\text{high organs}} = (\overline{A} - \overline{S})^2 + V_A + V_S \qquad (18a)$$

$$\text{Inaccuracy}_{\text{low organs}} = (\overline{a} - \overline{s})^2 + V_a + V_s \qquad (18b)$$

$$\text{Total Inaccuracy} = \\ \text{Inaccuracy}_{\text{high organs}} + \text{Inaccuracy}_{\text{low organs}} \qquad (19)$$

$$\text{Mean}\wedge2 - \text{Standardized Total Inaccuracy (M}^2\text{STI)} = \\ \frac{\text{Total Inaccuracy}}{\text{Population average organ height}^2} \qquad (20)$$

Inaccuracy at various dimensions is calculated as a linear deviation from the optimum in a two- or three-dimensional Euclidean space, making measurements comparable to one-dimensional inaccuracies. Hence, we adapted the inaccuracy index to multidimensional data by computing the Euclidean distance between average xyz coordinates of stigmas and stamens at each level in Eq. 18a and 18b:

$$\text{3Dinaccuracy}_{\text{high organs}} = \\ (\overline{x_A} - \overline{x_S})^2 + (\overline{y_A} - \overline{y_S})^2 + (\overline{z_A} - \overline{z_S})^2 + V_{3DA} + V_{3DS}$$

(21a)

$$\text{3Dinaccuracy}_{\text{low organs}} = \\ (\overline{x_a} - \overline{x_s})^2 + (\overline{y_a} - \overline{y_s})^2 + (\overline{z_a} - \overline{z_s})^2 + V_{3Da} + V_{3Ds}$$

(21b)

In these equations, the variance of each group of sex organs is defined from their Euclidean distances in the 3D space from their centroid (i.e., the mean of variances

for each dimension; for example, for stamens at level L, where N equals the number of individuals with stamens at level L):

$$V_{3DA} = \frac{1}{N}\left(\sum_{i=1}^{N}(x_i - \overline{x_A})^2 + (y_i - \overline{y_A})^2 + (z_i - \overline{z_A})^2\right) \tag{22}$$

Finally, total inaccuracy and mean²-standardized total inaccuracy in a 3D space are calculated as:

$$\text{3Dtotal Inaccuracy} =$$
$$\text{3Dinaccuracy}_{\text{high organs}} + \text{3Dinaccuracy}_{\text{low organs}} \tag{23}$$

$$\text{3DM}^2\text{STI} = \frac{\text{3Dtotal Inaccuracy}}{\text{PADO}^2} \tag{24}$$

where $PADO$ is the population average distance to the origin of all pooled sex organs, calculated as:

$$PADO = \frac{1}{T}\left(\sum_{i=1}^{T}\sqrt{x_i{}^2 + y_i{}^2 + z_i{}^2}\right) \tag{25}$$

where T equals the total number of sex organs measured.

In trimorphic populations, inaccuracy is also calculated for mid-level sex organs, and this contributes to total inaccuracy.

$$\text{3Dtotal Inaccuracy3M} = \text{3Dinaccuracy}_{\text{high organs}}$$
$$+ \text{3Dinaccuracy}_{\text{mid organs}} + \text{3Dinaccuracy}_{\text{low organs}} \tag{26}$$

$$\text{3DM}^2\text{STI3M} = \frac{\text{3Dtotal Inaccuracy3M}}{\text{PADO}^2} \tag{27}$$

Reciprocity vs. inaccuracy indices

Although both indices are highly correlated for distylous populations, the inaccuracy index of Armbruster et al. (2017) has to some extent replaced the reciprocity index of Sánchez et al. (2008, 2013) in recent years, based on two major criticisms. As Armbruster et al. (2017) depicted, (i) R incorporates measures of variation twice (both in r and in sdr), and (ii) the arbitrary multiplication of r by sdr (Eq. 6) implies that "even a large deviation from perfect reciprocity will have almost no effect on the total reciprocity if the standard deviation is close to zero." Furthermore, in contrast to variances, standard deviations are not additive and averaging them sensu Eq. 4 and 15 is problematic. We note, however, that Sánchez's r (sensu Eq. 3 for dimorphic populations and Eq. 16 for trimorphic) overcomes both shortcomings of Sánchez's R and is comparable across dimorphic and trimorphic populations. Using Sánchez's r may also be

appropriate in cases of polymorphic plants bearing intra-floral variation in the location of sex organs (e.g., Ferrero et al., 2011b; Turketti et al., 2012). Moreover, the multi-dimensional r index can be fairly applied to stylar polymorphisms including spatial and temporal dimensions (e.g., flexistyly; Li et al., 2001). Due to its additive nature, inaccuracy is not comparable across dimorphic and trimorphic populations and cannot directly apply to plants with intra-individual variation, but on the other hand, it allows the components of inaccuracy to be explored in depth. The R package FlowerMate provides tools for the most appropriate approach in each particular case, which will depend on the study system and objectives.

The FlowerMate R package

The R package FlowerMate v1.0 (Muñoz-Pajares and Simón-Porcar, 2024) is freely available in CRAN (see Data Availability Statement) and includes a function *inaccuracy* that computes either the one-, two-, or three-dimensional versions of the reciprocity and inaccuracy indices, either for dimorphic or trimorphic populations, depending on the data input and options chosen.

The input format includes one row per measured sex organ and the following eight columns: population code, floral morph (L, S, M, which may also be used for non-heterostylous morphs), individual ID number, sex organ ID number, sex organ type (stigma or anther), and x, y, z coordinates. The user can select the coordinates to compute, thereby obtaining either uni-, bi-, or three-dimensional indices. In multidimensional systems, this option also allows comparisons of reciprocity between various dimensions, which might provide insights into the differential strength of phenotypic selection. Some stylar polymorphic species present the same sex organs at strikingly different locations (e.g., unusual style-length polymorphic species with two stamen whorls instead of one, such as in *Narcissus* [Arroyo et al., 2002], or enantiostylous flowers with both left- and right-facing stamens [Johnson et al., 2023]), and for such cases *inaccuracy* offers the possibility to select different data subsets for computation. For polymorphisms that are not associated with heteromorphic incompatibility systems, it may also be interesting to test reciprocity within morphs to assess the potential contribution of intra-morph cross-mating (Johnson et al., 2023), and *inaccuracy* also offers this possibility. It may also be the case that missing data existed for some sex organs for at least one dimension. In such case, *inaccuracy* calculates both indices (in contrast to the Microsoft Excel macro of Sánchez et al., 2008, 2013), warning that the values may not be comparable across populations (e.g., if the distribution of missing data is strongly biased across morphs or dimensions).

The output of *inaccuracy* consists of a single table including the indices and their requested components for each population. Although we encourage the use of Sánchez's r (sensu Eq. 3, 12, and 16), FlowerMate also computes Sánchez's R (sensu Eq. 6 and 15), as it may be potentially

TABLE 2　Pearson's r correlation coefficients between the different components of the reciprocity index of Sánchez et al. (2008, 2013; Sánchez's r and Sánchez's R) and the inaccuracy index of Armbruster et al. (2017; total inaccuracy and mean^2-standardized inaccuracy) for dimorphic and trimophic populations simulated with FlowerMate and in *Pulmonaria* populations (Jacquemyn et al., 2018).

	Simulated dimorphic populations		Simulated trimorphic populations		*Pulmonaria* populations	
	Sánchez's r	Sánchez's R	Sánchez's r	Sánchez's R	Sánchez's r	Sánchez's R
Total inaccuracy	0.95***	−0.79***	0.91***	−0.86***	0.88***	−0.85***
Mean^2-STI	0.95**	−0.62**	0.74***	−0.53*	0.95***	−0.99**

Note: STI = standardized total inaccuracy. Significance: ***$P < 0.001$; **$P < 0.01$; *$P < 0.05$.

useful for researchers, for instance, for those interested in comparing their values to those published in previous studies. FlowerMate also includes functions that simulate style-polymorphic populations with the average coordinates and variance specified for each sex organ level and morph. These functions are *SimDimor* and *SimTrimor* for simulating dimorphic and trimorphic data, respectively.

Testing *inaccuracy* for one-dimensional data

First, we tested *inaccuracy* by replicating the one-dimensional reciprocity index retrieved with the Microsoft Excel macro of Sánchez et al. (2013) in two sets of 20 simulated populations, dimorphic and trimorphic, respectively. We used the functions *SimDimor* and *SimTrimor* in the FlowerMate package to simulate 20 dimorphic and 20 trimorphic populations with variable height mean differences between sex organs at each level and standard deviations. There was a perfect match between the reciprocity values retrieved with both approaches for both sets of populations, except for some very slight deviations that were attributed to the handling of decimal values (Appendices S1 and S2; see Supporting Information with this article). The computation of FlowerMate was notably faster than that of the Excel macro. From the values retrieved by FlowerMate, Sánchez's r (sensu Eq. 3; Sánchez et al., 2008) showed a stronger correlation than Sánchez's R (sensu Eq. 6; Sánchez et al., 2013) with both total inaccuracy and mean^2-standardized total inaccuracy (sensu Eq. 19 and 20; Armbruster et al., 2017) in dimorphic and trimorphic populations (Pearson's $r > 0.53$, $P < 0.05$; Table 2).

Second, we tested *inaccuracy* using the large database published by Jacquemyn et al. (2018), who calculated the inaccuracy index for 40 populations from nine distylous species of *Pulmonaria* (we excluded one duplicated population from their database [i.e., Crailsheim]). The value for all the components of the inaccuracy index retrieved with our code perfectly matched those published for most populations (Appendix S3). We attribute the mismatches found in a few populations to the improved handling of large amounts of data using our automated approach. For the values retrieved by FlowerMate, both Sánchez's R and r were significantly correlated with total inaccuracy and mean^2-standardized total inaccuracy ($r > 0.85$, $P < 0.001$; Table 2).

TABLE 3　Summary of dimorphic and trimorphic population sets representing different scenarios of increased phenotypic variation simulated to test the multidimensional variants of the reciprocity (Sánchez et al., 2008, 2013) and inaccuracy (Armbruster et al., 2017) indices.

Set	Description
Dimorphic populations	
Set 2D1	Increasing mismatch at x-axis, keeping total accuracy at y-axis
Set 2D2	Increasing variance at x-axis, keeping total accuracy at y-axis
Set 2D3	Increasing mismatch and variance at x-axis, keeping total accuracy at y-axis
Set 2D4	Increasing mismatch at x- and y-axes, with variances equal to 0
Set 2D5	Increasing variance at x- and y-axes
Set 2D6	Increasing mismatch and variance at x- and y-axes
Set 2D7	Increasing mismatch at x- and y-axes, with variances equal to 0.4
Set 2D8	Increasing mismatch and variance at x- and y-axes only at upper level
Set 2D9	Increasing mismatch and variance at x- and y-axes, x coordinates = y coordinates/2
Trimorphic populations	
Set 3D1	Increasing mismatch and variance at x-axis, keeping total accuracy at y- and z-axes
Set 3D2	Increasing mismatch and variance at x- and y-axes, keeping total accuracy at z-axis
Set 3D3	Increasing mismatch and variance at x-, y-, and z-axes

Testing *inaccuracy* for multidimensional data

First, we simulated 12 sets of five dimorphic populations that embodied different scenarios of increasing phenotypic variation in two or three dimensions. These population sets increased mismatch and/or variance in one or more dimensions while keeping the other components constant (Table 3, Appendices S4 and S5). Reciprocity and inaccuracy indices increased in all cases as expected (Figure 1).

Second, we tested *inaccuracy* using morphological data from 10 natural populations of *Linum suffruticosum* L. (Appendix S6), the first reported example of three-dimensional
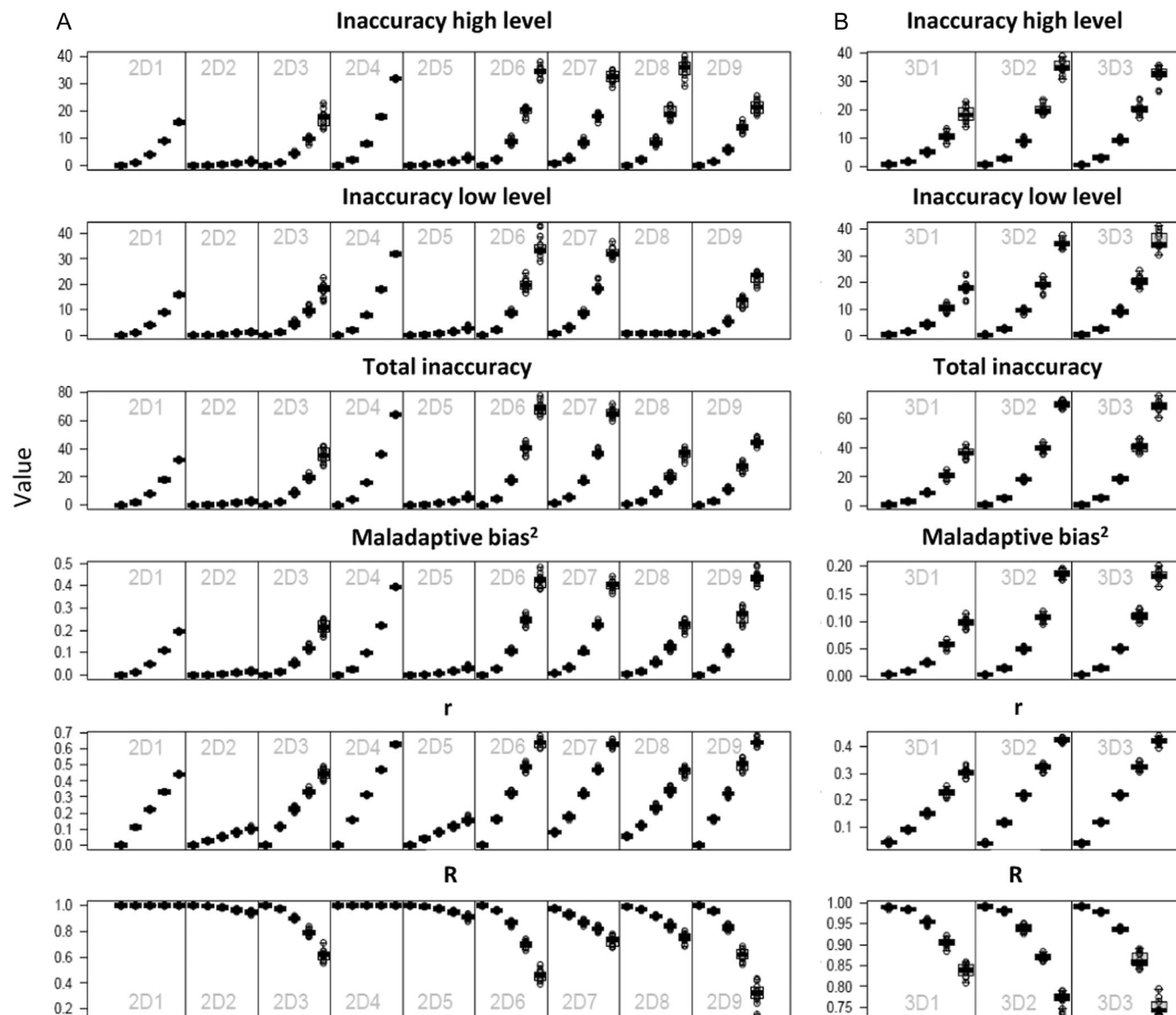
FIGURE 1 Components of the inaccuracy and reciprocity indices calculated with FlowerMate for 12 series of five populations representing different scenarios of increased phenotypic variation in the location of sex organs at two (A) or three (B) dimensions (see Table 3 for details).

heterostyly (Armbruster et al., 2006). Notably, although the locations of sex organs in this species occupy a three-dimensional space, the radial symmetry effectively entails two-dimensional functioning based on vertical and horizontal herkogamy, as pollinators visiting the flowers from any direction would contact sex organs in the same way. Previous authors (e.g., Armbruster et al., 2006; Pérez-Barrales and Armbruster, 2023) have analyzed reciprocity in this species by comparing the length of styles and filaments, but given their bending, such measurements do not correspond to the actual positioning of sex organs and may have little functional significance. Hence, xy coordinates are adequate to define the functional position of sex organs in this species and in other similar examples, and these can be easily obtained through measuring the height (y coordinate) and the diameter

($2x$ coordinate) of each sex whorl in fresh flowers. These measures can be obtained from scaled photos (Figure 2A) or, more easily, by using calipers. We used data for *Linum suffruticosum* to compare the reciprocity and inaccuracy indices retrieved with the xy coordinates and either the y or x coordinate. For the populations analyzed, we found a much higher variation along the y-axis than along the x-axis, which translated into a higher correlation between the values computed for xy and y data ($r > 0.94$, $P < 0.001$) than for xy and x data ($r < 0.51$, $P > 0.1$; Appendix S6). These results indicate that in this study system the height of sexual organs is a good predictor of two-dimensional reciprocity, which may not be the case in all study systems.

Finally, we tested *inaccuracy* with three-dimensional data using morphological data from one natural population

FIGURE 2   Representation of the coordinate calculations for sex organs in two-dimensional (A; e.g., *Linum suffruticosum*, short-styled morph) and three-dimensional (B; e.g., *Wachendorfia paniculata*, left-handed morph) systems. White lines represent the reference system, with the origin established at the level of the nectaries. Stigma coordinates are represented in each system by red lines, and anther coordinates by light green, dark green, and blue lines.

of the enantiostylous plant *Wachendorfia paniculata* L. (Haemodoraceae). Three-dimensional data are appropriate for zygomorphic flowers, which pollinators always approach from the same direction, and enantiostylous species present a typical case. Enantiostylous flowers in the Haemodoraceae bear one style and one stamen facing one side (either left- or right-handed) and two stamens, one longer that the other, facing the opposite side. We used front- and top-scaled photographs of freshly opened flowers of *W. paniculata* to retrieve the *xyz* coordinates of each sex organ in each morph (Figure 2B, Appendix S7) using the nectaries as the origin. We used this dataset to compare the three-dimensional reciprocity and inaccuracy indices using each of the three existing anthers (Figure 2B). As expected, the reciprocity was highest for anther 1 (Sánchez's $r_{3D} = 0.37$, 3DM^{2}STI $= 0.173$), intermediate for anther 2 (Sánchez's $r_{3D} = 0.606$, 3DM^{2}STI $= 0.426$), and lowest for anther 3 (Sánchez's $r_{3D} = 1.326$, 3DM^{2}STI $= 1.817$). Sánchez's r_{3D} and 3DM^{2}STI showed a high correlation across the three calculations (Pearson's $r = 0.995$, $P = 0.061$).

CONCLUSIONS

Multidimensional variants expand the range of applications of the existing reciprocity (Sánchez et al., 2008, 2013) and inaccuracy (Armbruster et al., 2017) indices that have been applied to heterostylous species. We have illustrated their potential application to various kinds of reciprocal stylar polymorphisms, and moreover, we advocate for their potential use in the characterization of other types of reciprocal polymorphisms maintained through disassortative mating (Armbruster et al., 2017). These may also include a temporal dimension (e.g., heterodichogamy; Renner, 2001) and may even be applied to animal populations (e.g., Schilthuizen et al., 2007; Takahashi and Hori, 2008). FlowerMate provides easy and fast computation of unidimensional and multidimensional indices. This new tool is designed to facilitate understanding of the evolution and function of the full diversity of reciprocal polymorphisms.

AUTHOR CONTRIBUTIONS

DATA AVAILABILITY STATEMENT

The data used to test the code are available as Supporting Information or from the source articles. The R package is available on CRAN (https://CRAN.R-project.org/package=FlowerMate).

ORCID

Violeta Simón-Porcar http://orcid.org/0000-0003-4024-2824

REFERENCES

Armbruster, W. S., R. Pérez-Barrales, J. Arroyo, M. E. Edwards, and P. Vargas. 2006. Three-dimensional reciprocity of floral morphs in wild flax (*Linum suffruticosum*): A new twist on heterostyly. *New Phytologist* 171: 581–590.

Armbruster, W. S., T. F. Hansen, C. Pélabon, R. Pérez-Barrales, and J. Maad. 2009a. The adaptive accuracy of flowers: Measurement and microevolutionary patterns. *Annals of Botany* 103: 1529–1545.

Armbruster, W. S., T. F. Hansen, C. Pélabon, and G. H. Bolstad. 2009b. Macroevolutionary patterns of pollination accuracy: A comparison of three genera. *New Phytologist* 183: 600–617.

Armbruster, W. S., G. H. Bolstad, T. F. Hansen, B. Keller, E. Conti, and C. Pélabon. 2017. The measure and mismeasure of reciprocity in heterostylous flowers. *New Phytologist* 215: 906–917.

Arroyo, J., S. C. H. Barrett, R. Hidalgo, and W. W. Cole. 2002. Evolutionary maintenance of stigma-height dimorphism in *Narcissus papyraceus* (Amaryllidaceae). *American Journal of Botany* 89: 1242–1249.

Barrett, S. C. H. 2002. The evolution of plant sexual diversity. *Nature Reviews Genetics* 3: 274–284.

Barrett, S. C. H. 2019. 'A most complex marriage arrangement': Recent advances on heterostyly and unresolved questions. *New Phytologist* 224: 1051–1067.

Braga, B. L. P., R. Matias, H. Consolaro, J. T. Souza, and N. M. Almeida. 2022. Inaccuracy of sexual organ position and spatial variation of styles in monomorphic enantiostylous flowers of *Senna rugosa* (Fabaceae-Caesalpinioideae). *Flora* 293: 152112.

Brys, R., and H. Jacquemyn. 2020. The impact of individual inaccuracy of reciprocal herkogamy on legitimate pollen deposition and seed set in a distylous self-incompatible herb. *Journal of Ecology* 108: 81–93.

Cresswell, J. E. 1998. Stabilizing selection and the structural variability of flowers within species. *Annals of Botany* 81: 463–473.

Darwin, C. 1877. The different forms of flowers on plants of the same species. John Murray, London, United Kingdom.

Eckert, C. G., and S. C. H. Barrett. 1994. Tristyly, self-compatibility and floral variation in *Decodon verticillatus* (Lythraceae). *Biological Journal of the Linnean Society* 53: 1–30.

Faife-Cabrera, M., V. Ferrero, and L. Navarro. 2014. Unravelling the stylar polymorphism in *Melochia* (Malvaceae): Reciprocity and ancillary characters. *Botanical Journal of the Linnean Society* 176: 147–158.

Faife-Cabrera, M., V. Ferrero, and L. Navarro. 2018. Relationship between herkogamy, incompatibility and reciprocity with pollen–ovule ratios in *Melochia* (Malvaceae). *Plant Biosystems* 152: 80–89.

Fenster, C. B. 1991. Selection on floral morphology by hummingbirds. *Biotropica* 23: 98–101.

Ferrero, V., S. Castro, J. M. Sánchez, and L. Navarro. 2011a. Stigma–anther reciprocity, pollinators, and pollen transfer efficiency in populations of heterostylous species of *Lithodora* and *Glandora* (Boraginaceae). *Plant Systematics and Evolution* 291: 267–276.

Ferrero, V., I. Chapela, J. Arroyo, and L. Navarro. 2011b. Reciprocal style polymorphisms are not easily categorised: The case of heterostyly in *Lithodora* and *Glandora* (Boraginaceae). *Plant Biology* 13: 7–18.

Fisher, R. A. 1958. The genetical theory of natural selection. Dover Publications, New York, New York, USA.

Fox, C. W., D. A. Roff, and D. J. Fairbairn. 2001. Evolutionary ecology: Concepts and case studies. Oxford University Press, Oxford, United Kingdom.

Ganguly, S., and D. Barua. 2021. Inter-morph pollen flow and reproductive success in a self-compatible species with stigma-height dimorphism: The influence of herkogamy and reciprocity. *Plant Biology* 23: 939–946.

Ganguly, S., P. M. Shreenidhi, and D. Barua. 2021. Increased variation in sex organ positions can increase reciprocity and pollination success in heterostylous plant populations. *Plant Species Biology* 36: 463–475.

Harley, R. M., A. M. Giulietti, I. S. Abreu, C. Bitencourt, F. F. D. Oliveira, and P. K. Endress. 2017. Resupinate dimorphy, a novel pollination strategy in two-lipped flowers of *Eplingiella* (Lamiaceae). *Acta Botanica Brasilica* 31: 102–107.

Jacquemyn, H., M. Gielen, and R. Brys. 2018. Is sexual organ reciprocity related to legitimate pollen deposition in distylous *Pulmonaria* (Boraginaceae)? *Oikos* 127: 1216–1224.

Johnson, S. D., J. J. Midgley, and N. Illing. 2023. The enantiostylous floral polymorphism of *Barberetta aurea* (Haemodoraceae) facilitates wing pollination by syrphid flies. *Annals of Botany* 132: 1107–1118.

Lande, R., and S. J. Arnold. 1983. The measurement of selection on correlated characters. *Evolution* 37: 1210–1226.

Li, Q., Z. Xu, Y. Xia, L. Zhang, X. Deng, and J. Gao. 2001. Study on the flexistyly pollination mechanism in *Alpinia* plants (Zingiberaceae). *Acta Botanica Sinica* 43: 364–369.

Massinga, P. H., S. D. Johnson, and L. D. Harder. 2005. Heteromorphic incompatibility and efficiency of pollination in two distylous *Pentanisia* species (Rubiaceae). *Annals of Botany* 95: 389–399.

Minnaar, C., and B. Anderson. 2021. A combination of pollen mosaics on pollinators and floral handedness facilitates the increase of outcross pollen movement. *Current Biology* 31: 3180–3184.

Muñoz-Pajares, A. J., and V. Simón-Porcar. 2024. FlowerMate: Reciprocity indices for style-polymorphic plants. R package version 1.0. https://cran.r-project.org/web/packages/FlowerMate/index.html [accessed 19 September 2024].

Oliveira, L. C., R. Matias, M. T. Furtado, R. Romero, and V. L. G. de Brito. 2022. What explains the variation in length of stamens and styles in a pollen flower? A study exemplified by *Macairea radula* (Melastomataceae). *Plant Systematics and Evolution* 308: 15.

Pauw, A. 2005. Inversostyly: A new stylar polymorphism in an oil-secreting plant, *Hemimeris racemosa* (Scrophulariaceae). *American Journal of Botany* 92: 1878–1886.

Pélabon, C., W. S. Armbruster, T. F. Hansen, G. H. Bolstad, and R. Pérez-Barrales. 2012. Adaptive accuracy and the adaptive landscape. In E. Svensson and R. Calsbeek [eds.], The adaptive landscape in evolutionary biology, 150–168. Oxford University Press, Oxford, United Kingdom.

Pérez-Barrales, R., and W. S. Armbruster. 2023. Incomplete partitioning of pollinators by *Linum suffruticosum* and its coflowering congeners. *American Journal of Botany* 110: e16181.

Rech, A. R., M. T. Achkar, L. R. Jorge, W. S. Armbruster, and O. J. Almeida. 2020. The functional roles of 3D heterostyly and floral visitors in the reproductive biology of *Turnera subulata* (Turneroideae: Passifloraceae). *Flora* 264: 151559.

Renner, S. S. 2001. How common is heterodichogamy? *Trends in Ecology & Evolution* 16: 595–597.

Richards, J. H., and S. Koptur. 1993. Floral variation and distyly in *Guettarda scabra* (Rubiaceae). *American Journal of Botany* 80: 31–40.

Sánchez, J. M., V. Ferrero, and L. Navarro. 2008. A new approach to the quantification of degree of reciprocity in distylous (sensu lato) plant populations. *Annals of Botany* 102: 463–472.

Sánchez, J. M., V. Ferrero, and L. Navarro. 2013. Quantifying reciprocity in distylous and tristylous plant populations. *Plant Biology* 15: 616–620.

Schilthuizen, M., P. G. Craze, A. S. Cabanban, A. Davison, J. Stone, E. Gittenberger, and B. J. Scott. 2007. Sexual selection maintains whole-body chiral dimorphism in snails. *Journal of Evolutionary Biology* 20: 1941–1949.

Simón-Porcar, V. I., A. J. Muñoz-Pajares, A. de Castro, and J. Arroyo. 2022. Direct evidence supporting Darwin's hypothesis of cross-pollination promoted by sex organ reciprocity. *New Phytologist* 235: 2099–2110.

Takahashi, T., and M. Hori. 2008. Evidence of disassortative mating in a Tanganyikan cichlid fish and its role in the maintenance of intrapopulation dimorphism. *Biology Letters* 4: 497–499.

Thompson, J. D., A. C. Cesaro, and J. Arroyo. 2012. Morph ratio variation and sex organ reciprocity in style-dimorphic *Narcissus assoanus*. *International Journal of Plant Sciences* 173: 885–893.

Turketti, S. S., K. J. Esler, and L. L. Dreyer. 2012. Three-dimensional reciprocity: A new form of tristyly in South African *Oxalis* (Oxalidaceae) species and its implications for reproduction. *South African Journal of Botany* 78: 195–202.

SUPPORTING INFORMATION

Additional supporting information can be found online in the Supporting Information section at the end of this article.

Appendix S1. Inaccuracy and reciprocity values retrieved from FlowerMate for 20 simulated dimorphic populations, and the *R* values obtained using the Microsoft Excel macro of Sánchez et al. (2008, 2013).

Appendix S2. Inaccuracy and reciprocity values retrieved from FlowerMate for 20 simulated trimorphic populations, and the *R* values obtained using the Microsoft Excel macro of Sánchez et al. (2008, 2013).

Appendix S3. Inaccuracy values published in Jaquemyn et al. (2018) for 39 populations of *Pulmonaria*, and inaccuracy and reciprocity values obtained with FlowerMate.

Appendix S4. Parameters used to simulate nine sets of five dimorphic populations with two-dimensional variation in the location of sex organs.

Appendix S5. Parameters used to simulate three sets of five dimorphic populations with three-dimensional variation in the location of sex organs.

Appendix S6. Two-dimensional data, and inaccuracy and reciprocity values retrieved from FlowerMate when computing either the xy, x, or y coordinates, in 10 populations of *Linum suffruticosum*.

Appendix S7. Three-dimensional data, and inaccuracy and reciprocity values retrieved from FlowerMate when computing either anther 1, anther 2, or anther 3, in a population of *Wachendorfia paniculata*.